frontiers | Frontiers in Transplantation

TYPE Original Research
PUBLISHED 17 November 2023
DOI 10.3389/frtra.2023.1257029

OPEN ACCESS

EDITED BY
Andrew R. Pepper,
University of Alberta, Canada

REVIEWED BY
Hirotake Komatsu,
Diabetes & Metabolism Research Institute, Beckman Research Institute, United States
Kuang-Ming Shang,
California Institute of Technology, United States

*CORRESPONDENCE
Klearchos K. Papas
✉ kkpapas@surgery.arizona.edu

†These authors have contributed equally to this work

‡Deceased

RECEIVED 11 July 2023
ACCEPTED 20 October 2023
PUBLISHED 17 November 2023

CITATION
Einstein SA, Steyn LV, Weegman BP, Suszynski TM, Sambanis A, O'Brien TD, Avgoustiniatos ES, Firpo MT, Graham ML, Janecek J, Eberly LE, Garwood M, Putnam CW and Papas KK (2023) Hypoxia within subcutaneously implanted macroencapsulation devices limits the viability and functionality of densely loaded islets.
Front. Transplant. 2:1257029.
doi: 10.3389/frtra.2023.1257029

Hypoxia within subcutaneously implanted macroencapsulation devices limits the viability and functionality of densely loaded islets

Samuel A. Einstein[1,2†], Leah V. Steyn[3†], Bradley P. Weegman[1,4†], Thomas M. Suszynski[5], Athanassios Sambanis[6], Timothy D. O'Brien[7,8], Efstathios S. Avgoustiniatos[3], Meri T. Firpo[8‡], Melanie L. Graham[7,9], Jody Janecek[9], Lynn E. Eberly[10], Michael Garwood[1], Charles W. Putnam[3] and Klearchos K. Papas[3*]

[1]Center for Magnetic Resonance Research, Department of Radiology, University of Minnesota, Minneapolis, MN, United States, [2]Department of Radiology, The Pennsylvania State University, Hershey, PA, United States, [3]Department of Surgery, University of Arizona, Tucson, AZ, United States, [4]Sylvatica Biotech Inc., North Charleston, SC, United States, [5]Department of Plastic Surgery, University of Texas Southwestern Medical Center, Dallas, TX, United States, [6]Department of Chemical & Biomolecular Engineering, Georgia Institute of Technology, Atlanta, GA, United States, [7]Veterinary Population Medicine Department, University of Minnesota, Saint Paul, MN, United States, [8]Department of Medicine, Stem Cell Institute, University of Minnesota, Minneapolis, MN, United States, [9]Department of Surgery, Preclinical Research Center, University of Minnesota, Saint Paul, MN, United States, [10]Division of Biostatistics, University of Minnesota, Minneapolis, MN, United States

Introduction: Subcutaneous macroencapsulation devices circumvent disadvantages of intraportal islet therapy. However, a curative dose of islets within reasonably sized devices requires dense cell packing. We measured internal PO2 of implanted devices, mathematically modeled oxygen availability within devices and tested the predictions with implanted devices containing densely packed human islets.

Methods: Partial pressure of oxygen (PO2) within implanted empty devices was measured by noninvasive ^{19}F-MRS. A mathematical model was constructed, predicting internal PO2, viability and functionality of densely packed islets as a function of external PO2. Finally, viability was measured by oxygen consumption rate (OCR) in day 7 explants loaded at various islet densities.

Results: In empty devices, PO2 was 12 mmHg or lower, despite successful external vascularization. Devices loaded with human islets implanted for 7 days, then explanted and assessed by OCR confirmed trends proffered by the model but viability was substantially lower than predicted. Co-localization of insulin and caspase-3 immunostaining suggested that apoptosis contributed to loss of beta cells.

Discussion: Measured PO2 within empty devices declined during the first few days post-transplant then modestly increased with neovascularization around the device. Viability of islets is inversely related to islet density within devices.

KEYWORDS

islet transplantation, immunoisolation, fluorine-19, magnetic resonance spectroscopy, tissue engineering, hypoxia

1. Introduction

Islet replacement therapy remains a potential cure for type 1 diabetes (1–9). Despite recent improvements in islet transplantation, only about half of patients treated at the most experienced centers are insulin independent five years after transplantation (2–5, 10–19). The current standard for islet transplantation—the intraportal delivery of islets—is admittedly imperfect due to significant islet graft dysfunction and loss over time. Factors contributing to suboptimal engraftment in the liver include: blood-mediated reactions, resulting in inflammation and thrombus formation (20–23); recurrent autoimmunity (24); immunosuppressive drug-related cytotoxicity (25–33); and poor oxygenation (34–44). Importantly, cells transplanted into the liver are difficult to monitor for survival and function and are irretrievable (45–49). Because of the challenges and limitations imposed by intrahepatic transplantation of islets, there has been persistent interest in and a resurgence of investigational studies focused on developing extrahepatic tissue-engineered islet grafts, a "bioartificial pancreas" (50–55).

Although extrahepatic islet transplantation using tissue-engineered grafts (TEGs) obviates many of the limitations imposed by intraportal islet transplantation, the bioengineering, experimental, and clinical implementation of a TEG-based approach introduces its own challenges, including: (1) To avoid the necessity for systemic immunosuppression to protect allografted islets, the encapsulation strategy may incorporate an immunoisolation membrane; this prevents host immunomodulatory cells from gaining access to the islets. However, the unintended but unavoidable consequence of immunoisolation is to prevent host vascular penetration into the graft; biophysically, this distances the vasculature from the encapsulated islets, creating an additional hindrance to the rapid diffusion of gases and small molecules. The consequence is that delivery of oxygen and nutrients to the islets and the efflux of insulin and other effectors from the graft is to a degree impeded (50, 56–63). (2) Because transplantation of large numbers of islet equivalents (IE) based on body weight (>5,000 IE/kg) are needed to achieve insulin independence (64–66), grafts must be seeded at high densities in order to use devices of a reasonable size for patients (43, 57, 67–70). (3) The implantation site for the device is no less important; the optimal site would ensure proper access to nutrients and allow for efficient insulin secretion (59, 60). Many extrahepatic sites have been considered and investigated (38, 39, 47, 71–78) but the local partial pressures of oxygen (PO2) at these proposed sites is seldom reported, especially within TEGs. Adequate oxygenation is critical: the survival and especially the functionality of islets are highly sensitive to hypoxic or anoxic conditions (79–83). Accurate and precise monitoring of oxygenation status is therefore a critical parameter in the design and implementation of therapeutic TEGs.

This study investigated the effects of increasing islet density on the viability and function of TEGs implanted in either the subcutaneous space or the intraperitoneal cavity of inbred rats. Internal PO2 of sham (acellular) TEGs was measured using fluorine-19 magnetic resonance spectroscopy (^{19}F-MRS); this technique has been validated for the measurement of TEG PO2 *in vitro* and *in vivo* (84, 85). These measurements, at intervals over 29 days post implantation, were employed to inform a mathematical model constructed to predict the effects of PO2 external to a device loaded with high islet densities, on graft viability and function. The model was then challenged by loading TEGs with islets at various densities, then implanting them in athymic nude rats (to minimize immunological reactivity) for one week. The devices were then explanted and the viability of their cellular contents measured by oxygen consumption rate (OCR); the data obtained were compared to predictions from the mathematical model.

2. Methods

2.1. Ethics statement and experimental schema

All animal research was performed with the approval of and in accordance with guidelines of the University of Minnesota and the University of Arizona Institutional Animal Care and Use Committees (IACUC). Procurement of human islets was approved and overseen by the University of California Institutional Review Board and informed consent was obtained for all donors.

The experimental schema is described and illustrated in **Figure 1**.

2.2. Sham (acellular) tissue-engineered graft (TEG) construction

The contents of TEG constructs for ^{19}F-MRS were constituted as a matrix and protected within a clinically-established macroencapsulating immunoisolation device (TheraCyte Inc., Laguna Hills, CA, USA) (59, 86–92), a device chosen for its flexibility, biocompatibility, and published record of successful pre-clinical (86, 93–98) and clinical implementation (91). All implantation procedures were performed using sterile techniques, materials, and reagents.

Sham implants (without islets, $n = 9$) were loaded with equal volumes of porcine plasma (Sigma Aldrich, St. Louis, MO, USA) and perfluoro-15-crown-5-ether (PFCE) (Exfluor Research Corporation, Round Rock, TX, USA), a type of perfluorocarbon with high oxygen solubility. The emulsion was injected into a 40 μl immunoisolation device using a 250 µl precision syringe (Hamilton Company, Reno, NV, USA), then cross-linked with 5% v/v bovine thrombin solution. The latter was prepared by diluting concentrated topical thrombin solution (GenTrac Inc., Middleton, WI, USA) in phosphate-buffered saline with calcium and magnesium. After loading the TEG, the cell access port was trimmed and sealed with adhesive (Dermabond, Ethicon Inc., Somerville, NJ, USA).

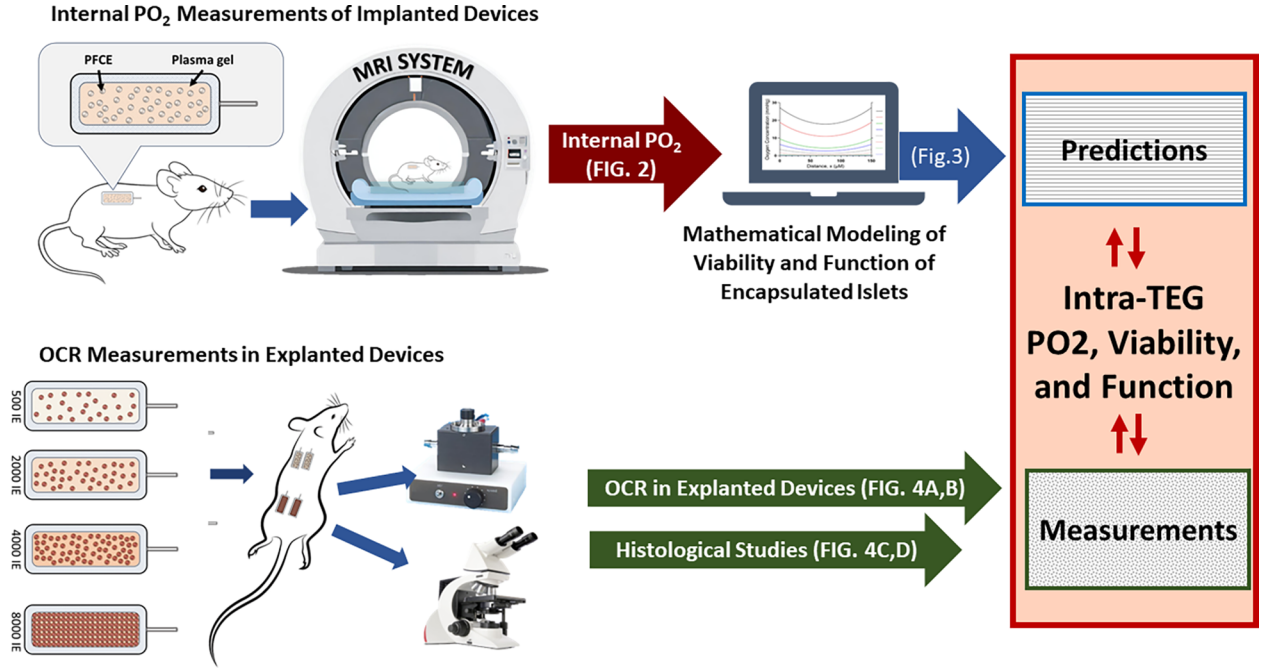

FIGURE 1
Schema for the experiments reported herein. Rats implanted with sham TEGs containing perfluoro-15-crown-5-ether (PFCE) and hydrogel, but without islets, were submitted to non-invasive fluorine-19 magnetic resonance spectroscopy (^{19}F-MRS) to measure the partial pressure of oxygen within the *in vivo* devices. The data obtained informed the mathematical model constructed to estimate graft viability and function for various islet graft densities. The model results were challenged by implanting islet-loaded TEGs at different densities and measuring their viabilities by OCR after explantation. The OCR values obtained were used to calculate fractional viability and functionality, the final outputs. All implanted TEGs were examined histologically after their removal.

2.3. Surgical implantation of sham TEGs

To measure the oxygenation status of TEGs *in vivo*, individual sham TEGs containing PFCE (see 2.2) were implanted in the subcutaneous space ($n = 6$) or the peritoneal cavity ($n = 3$) of non-diabetic Lewis rats (RT1^{l}, Charles River Laboratories International, Inc., Wilmington, MA, USA). Anesthesia was induced with isoflurane by inhalation and maintained by spontaneous ventilation of isoflurane (1%–3%). The surgical site was clipped of hair and the skin prepped with chlorhexidine or an equivalent antiseptic. For subcutaneous implants, a 1.5 cm dorsal incision was made just inferior to the scapulae and perpendicular to and symmetrical about the mid-line. Using gentle blunt dissection, a small pocket sufficient to accommodate the device was created. After rinsing the pocket with saline, the device was placed in the pocket. For peritoneal implants, a 1.5 cm incision was made through the anterior abdominal wall to expose the peritoneum. The TEG implant was gently introduced into the abdominal cavity and tacked to the peritoneum using non-absorbable sutures, taking care not to place the TEG directly beneath the incision. The abdominal fascia and skin were closed with absorbable suture and the incision sealed with surgical glue (Dermabond). For postoperative analgesia, a nonsteroidal anti-inflammatory drug (NSAID) (meloxicam 1 mg/kg) was administered by subcutaneous injection once daily for at least 3 days. Animals were monitored daily until the incision was fully healed. After completion of the study, anesthetized animals were euthanized by inhalation of 100% carbon dioxide.

2.4. ^{19}F-MRS oximetry

Oxygen measurements from implanted (see 2.3) TEGs containing PFCE (see 2.2) were acquired with a 16.4 tesla, horizontal-bore MRI system (Agilent Technologies, Santa Clara, CA, USA), Figure 1. Anesthesia was induced and maintained with inhaled isoflurane (1%–3%) in 47%–49% oxygen; the slight variations in oxygen content occurred as isoflurane flow was adjusted to maintain appropriate sedation. The rat was immobilized using a holder which centered the TEG over a 1.5 cm radius, custom-built, single-loop surface coil tuned to the ^{19}F resonance frequency (656.8 MHz). The holder was inserted into the MRI system for scanning, during which the body temperature of the rat was carefully stabilized at 37 ± 0.2°C, as measured with a rectal thermocouple and regulated with a forced-air heater. The spin-lattice relaxation rate constant (R_1) was measured using an inversion-recovery pulse sequence with adiabatic pulses. The inversion-recovery curve was fitted to the Bloch equation solution for longitudinal magnetization, using 3-parameter non-linear regression, with Graphpad-Prism software (Graphpad Software Inc., La Jolla, CA, USA). Each R_1 was measured in six replicates separated by 6 s intervals, to ensure complete relaxation between repetitions. The R_1 of each

measurement was converted to PO2 using the previously determined multiparametric calibration (84). *In vivo* PO2 was measured on days 1, 4, 8, 15, 22, and 29 postimplantation (Figure 2). It is important to note that *in vivo* PO2 values determined by ^{19}F-MRS oximetry represent average measurements across each device (84).

2.5. Histology

Sham TEGs were explanted from Lewis rats after 29 days, fixed in 10% buffered formalin for ≥24 h, transferred to 70% ethanol solution, and then embedded in paraffin wax for histology. Three 5 µm sections from separate portions of each explant were examined by an experienced pathologist to assess the degree of vascularization, the presence of foreign body reaction (FBR), and the extent of fibrosis in the adherent tissue surrounding the TEG. The degree of vascularization in the tissue surrounding each TEG was scored in blinded fashion on a scale from 0 to 3, where 0 = *avascular;* 1 = *minimal vascularity*; 2 = *moderate vascularity*; 3 = *extensive vascularity*. FBR was scored by examining the extent of inflammatory cell infiltrate composed of multinucleated inflammatory giant cells and macrophages but absent of lymphocytes and plasma cells; the extent was scored: 0 = *none;* 1 = *minimal;* 2 = *mild*; 3 = *mild/moderate;* 4 = *moderate;* 5 = *moderate/severe;* and 6 = *severe*. The degree of fibrosis was scored on the same scale as FBR by examining the density of fibrosis in the surrounding tissue.

2.6. Mathematical modeling of viability and functionality of densely loaded islets in TEGs

To elucidate the impact of external PO2 and cell density on TEG-contained islet viability and function, a diffusion-reaction oxygen transport model was developed, based on the size, shape, and dimensions of the devices employed in this study, using methods previously described (50, 63, 99–102). The dimensions for the TheraCyte devices used in the study are: 4.5 µl (17.5 mm × 7.0 mm × 2 mm) and 20.0 µl (22 mm × 11.2 mm × 3 mm). COMSOL Multiphysics software (COMSOL Inc., Stockholm, Sweden) was employed to develop a finite-element model describing the steady state, 1D diffusion-reaction condition, within a macroencapsulating TEG device. The TEG is modeled as a thin slab of oxygen-consuming tissue surrounded by the device membranes (Figures 3A,B). Oxygen diffusion into the device is described by the PO2 gradient between the exterior and interior of the implant and the permeability of the membrane (103). Transport of oxygen through the oxygen-consuming islet tissue is governed by two factors: diffusion through the tissue and oxygen consumption rate (OCR) of the tissue (63); an OCR of functioning, viable islets of 300 nmol/min/mg DNA (104) was used for this calculation. The model predicts the steady-state spatial oxygen concentration within the tissue content of TEGs containing densely packed islets (Figures 3C,D); from these oxygen concentrations, the fractional viability and functionality of the tissue within the central compartment of the device can be estimated (Figures 3E,F). We modeled a range of PO2 from 1 to 40 mmHg: a PO2 of 30 mmHg has been reported for *in vivo* tissues (103, 105–110); an external PO2 of 10 mmHg is congruent with the PO2 recorded within the sham TEG by ^{19}F-MRS, see 2.4 and 3.1. Islets were considered to have some impairment of function at a steady-state PO2 of 8 mmHg and increasing loss of function as the PO2 diminished further. The islets were deemed non-viable when the steady-state PO2 was ≤0.1 mmHg (111). The parameters, equations and results of the simulations for islet cells are given in detail in the Supplementary Information File 1, and in Figure 3.

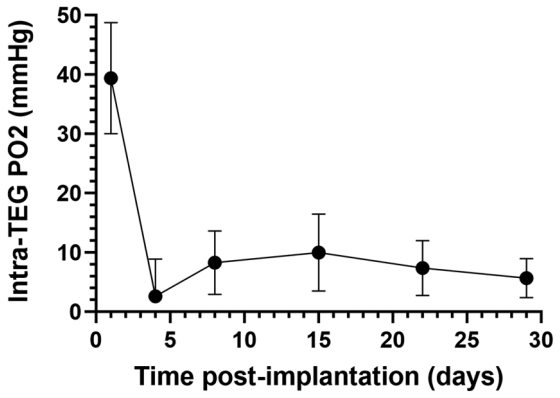

FIGURE 2
Oxygen partial pressure (PO2) measurements in subcutaneously implanted sham TEGs, as measured with non-invasive fluorine-19 magnetic resonance spectroscopy (^{19}F-MRS). Average PO2 of subcutaneously implanted sham TEGs ($N = 6$) were measured on days 1, 4, 8, 15, 22, and 29 post-implantation. The mean PO2 was significantly higher ($p < 0.0001$) on day 1 than any subsequent time point, but by day 4 the devices were profoundly hypoxic. Similar trends were observed at the intraperitoneal site (Supplemental Information Figures S1A and B).

2.7. Explant OCR measurements

To test the effects of islet density on viability *in vivo* within TEGs, implants containing various quantities of human islets were implanted in rats for 7 days and then explanted for OCR measurements (Figure 1). TEGs ($n = 19$) were of the same construction as the sham devices described above (see 2.2), except that they were loaded with islets. Human islets were isolated at the University of California, San Francisco, cultured at 22°C in supplemented CMRL culture medium for up to 14 days, and shipped to the University of Arizona in 10 cm^2 G-Rex devices (Wilson Wolf Manufacturing, New Brighton, MN, USA) (112, 113). Islets were quantified by DNA content (114–116) and aliquoted into tubes in various doses ranging from 500 to 8,000 IE per device. Each aliquot was then allowed to settle by gravity in its tube, the supernatant was removed, and the islets were re-suspended in 5 or 20 µl of sterile 1% sodium alginate solution. The islet suspension was then injected into the cell compartment of a 4.5 or 20 µl immunoisolation device, respectively, using a 100 µl precision syringe (Hamilton Company). The TEG was submerged in a 1.2 mM calcium chloride solution

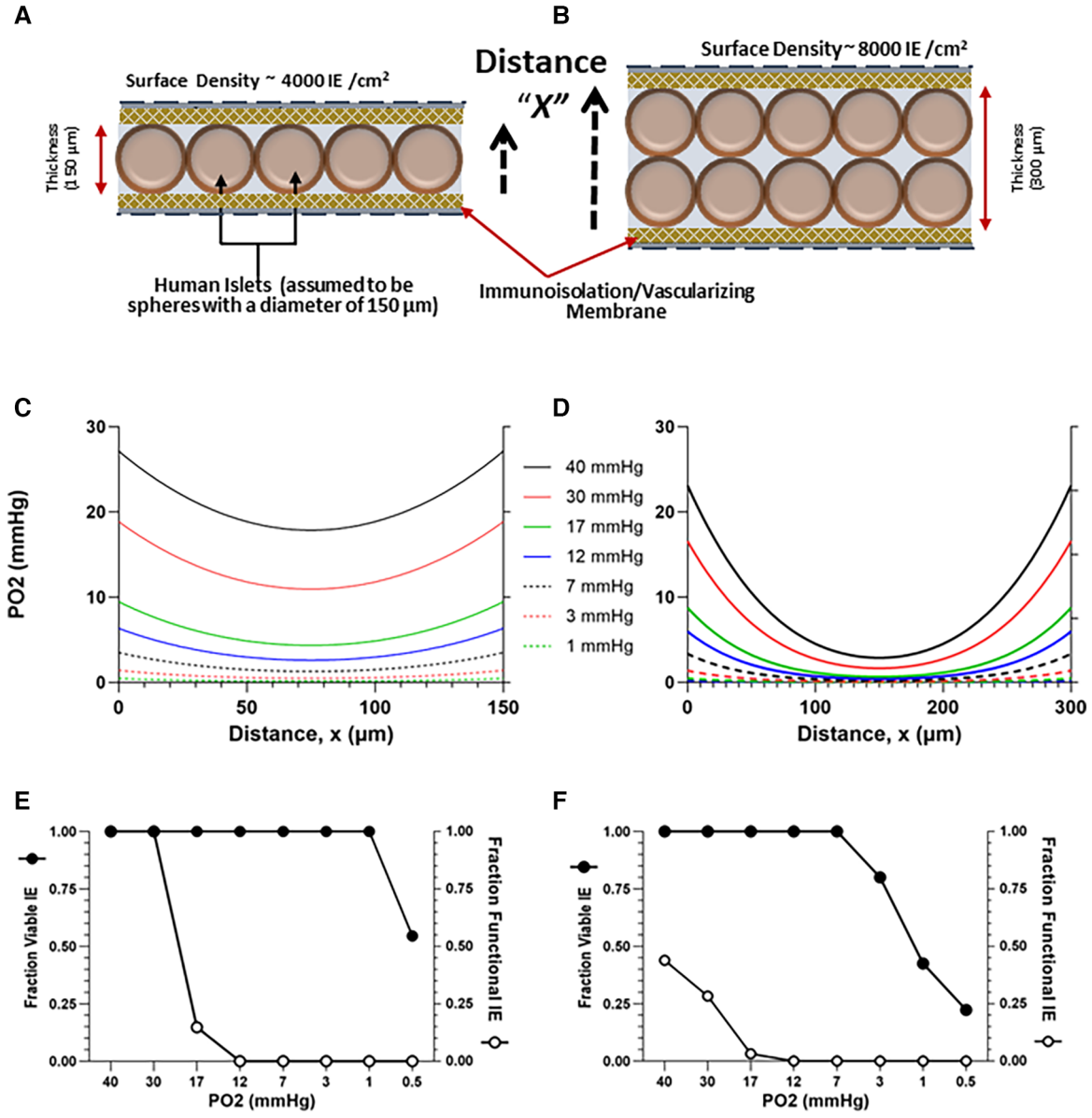

FIGURE 3
Model-estimated (see 1.6) oxygen profiles (C,D) and predicted viability and functionality (E,F) of human islets contained within TEGs at a planar-surface density of 4,000 or 8,000 IE/cm^2, assuming a homogenous slab of either of two thicknesses, 150 (A) and 300 (B) µM and external ambient PO2s ranging from 0.5 to 40 mmHg; the distance X plotted on the x-axis in (C,D) corresponds to the dashed arrows in (A,B). Thirty mmHg is a value commonly assumed in the literature and 10 mmHg is a value representative of the steady state derived from *in vivo* ^{19}F-MRS measurements (Figure 2). (E,F) Islet viability (threshold > 0.1 mmHg) and functionality (decreasing below 8 mmHg) are plotted against ambient PO2.

(PBS++) for 20–30 min to cross-link the alginate, then placed in PBS++ solution in preparation for implantation.

TEGs prepared with various doses of human islets were implanted in the subcutaneous space of 7 non-diabetic nude rats (athymic nude mutant, Hsd:RH-*Foxn1*^{rnu}, Harlan Laboratories, Inc, Indianapolis, IN, USA). Each rat received two to four devices, each separately placed in its own subcutaneous pocket. Seven days later, the TEGs were surgically removed for measurements of OCR to assess islet viability and for immunohistochemical staining. The surgical implantation and explantation procedures were identical to those described for sham TEGs (see 2.3).

The OCR of each explanted TEG was measured by a method similar to that described for the assessment of free islet viability (117). The surgically recovered TEGs were stripped of adherent surrounding tissue, placed in a modified OCR chamber, and filled with air-saturated cell culture medium. In the sealed chamber, the PO2 of the medium was continuously monitored until the values achieved a linear slope; the OCR was calculated from the slope. By normalizing the OCR to the number of IE originally loaded into each device, individual islet graft viability (OCR/IE) was calculated. Previous OCR data obtained *in vitro* of human islets in devices under ideal

conditions were used to calculate the "predicted OCR" at different densities (Figure 4A).

2.8. Immunohistochemistry of human islets in seven-day TEGs

TEGs containing various densities of human islets were explanted from nude rats after seven days, fixed in 4% paraformaldehyde and embedded in paraffin. Sections of 6 μm thickness were stained with DAPI (1 μg/ml, Roche, Indianapolis, IN, USA) or for insulin (guinea pig anti-porcine insulin 1:500, Dako, Carpinteria, CA, USA), and for cleaved caspase-3 (rabbit anti-human caspase-3, 1:250, Cell Signaling Technology, Danvers, MA, USA); detection was with affinity-purified secondary antiserum conjugated to donkey anti-rabbit IgG and donkey anti-guinea pig IgG (Alexa Fluor 488 and Alex Fluor 594, Jackson ImmunoResearch Laboratories, West Grove, PA, USA), as previously described (118). Independent images for each fluorophore were acquired using a Leica DM5500 microscope system, and the images were processed using Image Pro Plus 6.3 software (Media Cybernetics, Silver Spring, MD, USA); composite images were colored and assembled (blue = *DAPI*; red = *insulin*; green = *caspase-3*).

2.9. Statistical analysis

Average values are reported as the mean value and the standard error of the mean (SEM). Least squares-weighted-means and error values are reported for PO2 measurements due to large variabilities observed with some of the PO2 measurements. Statistical comparisons were performed with Graphpad-Prism software or SAS analysis package (version 9.2; SAS Institute, Cary, NC, USA).

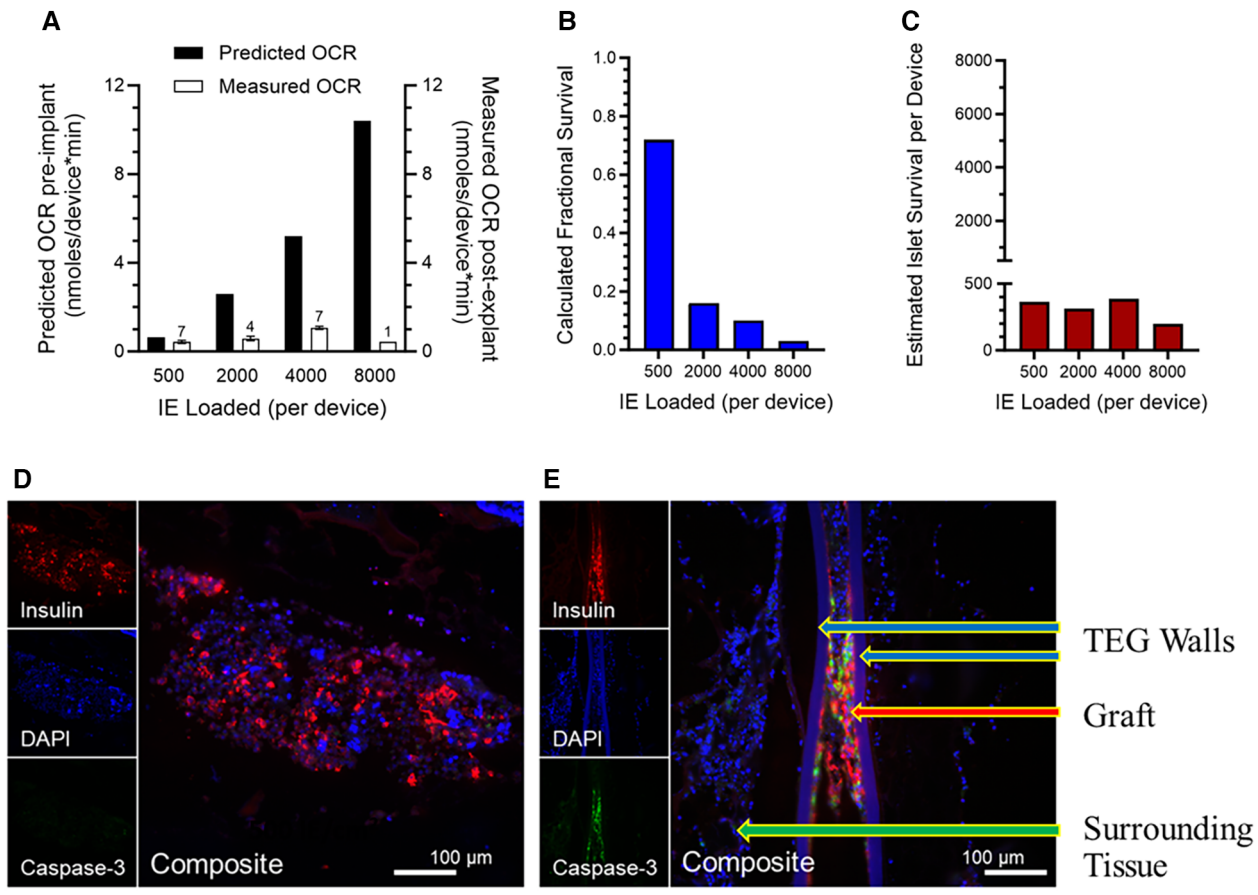

FIGURE 4
(**A**) Viability, measured by OCR of islets in explanted TEGs (*n* is given above the 'Measured OCR' columns), originally loaded with various densities and implanted in the SC space seven days previously; a dramatic decline in measured OCR in comparison to OCR predicted from the loading densities is observed with increasing islet density, far greater than that predicted by the mathematical model. (**B**) Fractional survival declined precipitously with increasing IE loading. (**C**) The absolute numbers of IE surviving number about 400 per device, regardless of the loading density. (**D**,**E**) Representative sections of the human islet cells within the same TEGs explanted after 7 days' residence in the subcutaneous space of nude rats. The tissues are stained with the nuclear stain DAPI (blue) or by immunohistochemistry for either the insulin (red) or caspase-3 (green) proteins (see 2.8 and 3.5). Two densities of human islets within TEGs are illustrated: (**D**) low density, 500 IE/cm^2, and (**E**) high density, 4,000 IE/cm^2. At the greater density, there are fewer viable cells (DAPI), less production of insulin, and prominent caspase-3 protein. The composite image at low density demonstrates viable islet cells producing insulin and devoid of caspase-3 whereas at the higher density caspase-3 co-localizes with the remaining insulin-producing cells, suggesting that apoptosis and necrosis of the islet cells have occurred. Labeled are the walls of the TEG, the islet cell graft within it, and the surrounding tissue.

3. Results

3.1. In vivo PO2 in empty subcutaneous and intraperitoneal TEGs

An important first step in modeling islet function and viability in TEGs was to obtain accurate measurements of oxygen concentrations within devices devoid of cells (see Figure 1). For this purpose, sham (acellular) TEGs loaded only with PFCE (2.2) were implanted in the subcutaneous space ($n = 6$) or peritoneal cavity ($n = 3$) of nine rats (2.3), monitored for 29 days using ^{19}F-MRS oximetry (2.4), then explanted for histologic examination (2.5). Internal PO2 measurements were successfully acquired in all animals at six time points (1, 4, 8, 15, 22, and 29 days) following implantation.

The average internal PO2 of subcutaneously implanted sham TEGs one day following implantation was 39 (SEM 9) mmHg (Figure 2), about that of venous blood (40 mmHg). The day 1 value however was the highest obtained; it was significantly greater ($p < 0.0001$) than all values at successive time points. By day 4, the PO2 had decreased nearly to zero and then increased but remained at very low levels (~10 mmHg) for the remainder of the time course. The same downward trend of PO2 over time was observed in the smaller set of IP implanted TEGs (Supplemental Information Figure S1A,B). A comparison of the PO2 values at each site on days 1 and 4 (Supplemental Information Figure S1A) were not statistically significantly different nor were the total time averaged PO2 values presented in Figure S1B, 12 (SEM 5) and 8 (SEM 10) mmHg for subcutaneous and intraperitoneal TEGs, respectively. Again, the difference was not statistically significant. It should be emphasized that the PO2 measurements using 19F-MRS oximetry of sham devices represent holistic measures of the entire TEG compartment, i.e., average values not limited to the boundary layer or other presumed sub compartments (84). Together, these data document that for at least the first month after implantation, the steady state partial pressure of oxygen within empty TEGs is in fact quite low, about 10 mmHg, in both the subcutaneous and intraperitoneal sites.

3.2. Histology of explanted sham TEGs

The low partial pressures of oxygen recorded within TEGs (see 3.1, above) may be the consequence of low blood vessel density around the empty devices and/or the presence of other oxygen consuming cells on the device surface, limiting oxygen transfer to its interior. Note that devices *containing cells* are reported to have increased densities of blood vessels around them, presumably due to pro-vascularization factors released by the implanted cells (119–122).

Hematoxylin and eosin-stained tissues surrounding explanted (day 29) *empty implants* from the immunocompetent Lewis rats were graded for successful vascularization and adverse fibrotic and foreign body reactions. Successful vascularization—an average score of 2.3 on a scale of 0 to 3—was evident; it was accompanied by only mild to moderate amounts of fibrosis (average score of 2.3/6) and a similar degree of foreign body reaction, average score of 2.7/6. Importantly, these mild responses are not to be confused with the fibrous encapsulation accompanying the traditional foreign body response (123) and were not directed toward the vascularizing membrane nor did they interfere with neovascularization at the device interface (124). This observation is in marked contrast to the classic host FBR observed in the absence of an appropriate vascularization membrane (125) or in reaction to SC LiPc-PDMS solid oxygen probes which were "enveloped by a fibrous capsule" after 6 weeks (126). Examination of the internal compartments of the TEGs showed remnants of the fibrin scaffold in all explants. No inflammatory cell infiltration was observed within the internal chamber of the TEGs, evidence that the immunoisolation chambers had not been breached. Thus, it appeared that TEGs remained intact for and were moderately-well vascularized by 29 days; images of explanted TheraCyte TEGs after 28 days residence in the host are shown in the Supplementary Information Figure S2). We conclude that host fibrotic and foreign body reactions, although observed, were mild in comparison to vascularization.

3.3. Predictions from the mathematical model of TEG oxygenation

Projections from the diffusion-reaction model of *in vivo* TEG oxygenation constructed *in silico* (see 2.6) to quantify the effects of implant site PO2 and islet cell density on TEG viability and function are presented in Figure 3. Curves for various oxygen concentrations external to the device are shown for cell layers of 4,000 (Figure 3A) and 8,000 (Figure 3B) IEQ/mL, in devices measuring 150 or 300 μM thickness, respectively, Figures 3C,D; the higher PO2 values are commensurate with assumptions often made in the literature (see Introduction); the lower PO2 values are representative of the data from *in vivo* ^{19}F-MRS oximetry, described earlier (see 3.1).

Viability [which has a threshold of 0.1 mmHg (111)] was not affected in the thinner layer model by decreasing the external oxygen concentration (Figure 3E), except at the very lowest oxygen concentration (0.5 mmHg). However, the proportion of viable cells decreased at 3 mmHg in the 300 μM thickness model (Figure 3F).

As anticipated, the model predicts a far more dramatic decline in graft function [which is known to be compromised at ~8 mmHg (57, 127) or lower, see 2.6], a much higher threshold than viability. In the thinner cell slab model (150 μM), loss of function by about 85% is predicted at an external PO2 of 17 mmHg; at 12 mmHg, nonfunctionality of all islets is anticipated (Figure 3F). In the 300 μM model, nonfunction of the majority of cells is predicted even at a 40 mmHg oxygen concentration (Figure 3F). The mathematical model thus predicts that, for a PO2 of 30 mmHg (the upper limit of previously expected values) and a planar-surface density of 4,000 IE/cm^2, functionality remains intact in a thinner device but is severely compromised in the thicker device. Importantly, at the measured oxygen content of empty TEGs, namely ~10 mmHg (see 3.1), the predicted functionality is essentially null under the conditions of the model (Figures 3E,F).

3.4. Estimation of viability of explanted TEG islet grafts by oxygen consumption rate

In light of the low internal PO2 of~10 mmHg measured in TEGs (see 3.1) despite histologic evidence of successful vascularization (see 3.2 and Supplemental Information Figure S2), and the consequent results from the mathematical model (see 3.3) of severe loss of functionality with a PO2 of 10 mmHg, we sought data challenging the predictions posited by the model.

For this purpose, 19 immunoisolation TEGs of identical design to the sham TEGs were loaded with various numbers (determined by DNA content) of human islets suspended in alginate, then implanted subcutaneously in 7 nondiabetic nude rats; each rat received 2–4 devices in separate locations (see 2.7 and Figure 1). Seven days after implantation, the TEGs were surgically removed, stripped of adherent tissue, and placed in an OCR chamber for measurements of oxygen consumption rate (see 2.7). OCR was normalized to the number of IE loaded into each device and the individual islet graft viability (OCR/IE) was calculated. Logistically, it was not possible to measure OCR prior to implantation because of the attendant risk of infection after implantation. Instead, we used prior data from a study of OCR *ex vivo* of human islets in similar devices under ideal conditions; from these data, the predicted OCR for each density was calculated (Figure 4A).

As the model (Figure 3) had predicted, the measured viability (% viable tissue) decreased with increasing islet density at a pronounced rate, especially at low and moderate densities (Figure 4A). The calculated fractional survival likewise decreased with increasing IE loads; it was less than 20% for all densities except the lowest (Figure 4B). The estimated islet (IE) survival was also calculated (IE loaded*fractional survival); it was below 400 IE/device, even when 8,000 IE were loaded (Figure 4C).

Thus, the mathematical model portrayed trends in functionality and viability with accuracy; importantly, however, measured viability—especially at higher densities—did not meet the predicted rates and fell more precipitously than predicted by the mathematical model. This is consistent with the values measured on day 4 post implant (Figure 2) being well below the 10 mmHg measured at steady state when neovascularization had presumably occurred. In other words, until functional blood vessels are created, the cells that surround the device may deplete oxygen, lowering the intra-device PO2 to near zero until newly formed, functional vessels begin transporting oxygen-bearing RBCs to the area.

3.5. Immunohistochemistry of insulin and caspase-3 in explanted TEGs loaded with islets

To better understand the fate of islet cells at higher densities in TEGs, the devices retrieved from nude rats at 7 days for the *ex vivo* OCR viability study described above (3.4) were studied with immunohistochemistry identifying insulin or the caspase-3 protein, a marker of apoptotic activity (see 2.8). Representative images from TEGs loaded with low-density (500 IE/cm^2) or high-density (≥2,000 IE/cm^2) human islets are shown in Figures 4D,E). At low density, the islet cells displayed staining for insulin and minimal if any caspase-3 protein (Figure 4D) whereas sections from high-density TEGs exhibited more caspase-3 protein, which co-localized with the residual staining of the insulin protein (Figure 4E). Consequently, we were able to confirm that human islets loaded at higher densities within subcutaneous TEG implants indeed quickly lose viability, at least in part through apoptotic mechanisms, as well as coincident and subsequent necrosis.

4. Discussion

The intent of this study was to determine whether immunoisolating tissue engineered grafts (TEGs) implanted subcutaneously or intraperitoneally in rats would be successfully vascularized; and, if so, would they have ambient partial pressures of oxygen (PO2) sufficient to support both viability and importantly, the functionality of islet grafts of various densities contained therein. We conclude that even modest densities of islets are not functionally sustainable within such implanted TEGs.

One corollary of this conclusion is that in order for islet grafts to survive and function within encapsulated devices such as TEGs, they must be loaded at very low cellular densities (128, 129) – an unacceptable solution since TEGs of a clinically useful size would not accommodate sufficient islets to reverse diabetes. An alternative, and far more appealing corollary, is that islet grafts can be sustained at high densities in reasonably sized devices, *if* the chambers of the devices are supplemented with oxygen at super-ambient partial pressures (79, 128, 130, 131). In immunoisolating or similar encapsulating TEGs, supplemental oxygen might well be a permanent requirement; nonimmunoisolating devices—having more porous membranes which allow ingrowth of neovasculature—might achieve the necessary internal oxygen content within weeks to months, thus allowing cessation of supplemental oxygen. Various laboratories have developed novel approaches for providing increased oxygenation to encapsulated islets (53, 70, 79, 132–136).

Our conclusion regarding the inadequacy of oxygenation of the TEG internal environment was based upon both *in vivo* experimental studies and *in silico* mathematical modelling of the devices (Figure 1). First, using ^{19}F-MRS oximetry of subcutaneously or intraperitoneally implanted sham TEGs, devoid of cells but containing PFCE, an average available PO2 of 12 (SEM 5) mmHg was measured for the SC site and only 6.8 (SEM 10) mmHg in the peritoneal space, after just a few days *in vivo* (Figure 2 and Supplementary Information Figure S2). At equilibrium *in vivo*, these measurements within sham (empty) devices can perhaps best be interpreted to represent the PO2 surrounding the implanted device, that is, the expected limit of oxygen available for transport into the device. Recently reported

PO2 measurements with a solid, totally implantable probe yielded roughly comparable values and somewhat similar trends for the native SC tissue and IP cavity (126). Importantly, the internal PO2 available to islets within the TEG would perforce be lower than these measured values due to oxygen consumption by the islets themselves, with the lowest oxygen concentrations in the center of the device. At higher planar-surface densities, the available PO2 would be considerably lower, perhaps effectively anoxic, because the oxygen consumption rate of islet cells further sharpens the oxygen gradient. Examples of this limitation are widely reported in the literature and have recently been reviewed (128). We emphasize that these unanticipated low values were not the consequence of excessive fibrosis or foreign body reaction, as was confirmed by histologic examination; the devices were in fact well vascularized (**Supplementary Information Figure S2**).

Because the *in vivo* oxygen levels of implanted sham TEGs were monitored for a 29-day period following implantation, the dynamics of the changing PO2 portrayed in **Figure 2** and **Supplementary Information Figure S1A** invite scrutiny. The PO2 on the first day following implantation was significantly higher than that recorded at all future time-points, likely due to the continued presence of residual oxygen in the TEGs (introduced during the preparation of the device at ambient PO2∼150 mmHG) and the surrounding surgical site. Then, a dramatic decrease in PO2, reaching near-zero levels, was observed (day 4). This is likely attributable to the recruitment of highly metabolic inflammatory cells to tissue damage at the surgical site. These cells not only compete for available oxygen but might also affect the graft indirectly though paracrine signaling and the local secretion of inflammatory cytokines; these possible effects were not addressed in our study. From days 8 to 22, we note a gradual, modest increase in PO2 within the devices; we hypothesize that this is the consequence of neovascularization in the SC or IP tissues surrounding the implanted TEG, slightly increasing the available oxygen. For the remaining 22–29 days following implantation, the ambient oxygenation appears to achieve a steady state. However, this vascular formation is insufficient to alleviate the hypoxic condition inside the immunoisolated TEG, especially when high densities of islets are required.

Mathematical modeling based on a range of external PO2s encompassing both 30 mmHg (a previously accepted oxygen concentration within sham devices) and 10 mmHg (representing our *in vivo* measurements) produced viability curves which were calculated with a threshold of 0.1 mmHg; the curves indicate that viability is sustainable at a moderate (4,000 IEQ/cm^2) planar-surface density. Functionality, however, poses a stark contrast to viability: with a ∼100-fold higher oxygen requirement than viability, functionality is likely already declining at 8 mmHg and is projected to be unacceptable at *any* islet density when modeling the 10 mmHg environment (**Figures 4E,F**). The mathematical model for predicting viability based on the PO2 available within TEGs is limited by its initial assumptions that vary depending on the specific environment *in vivo* (*e.g.*, factors beyond hypoxia and anoxia may contribute to graft loss) and are influenced by the characteristics of the particular islet preparations used for actual TEGs. Recognizing the limitations of mathematical modeling, experimental studies are required to evaluate any model's predictive reliability.

The dire predictions of the model were confirmed experimentally by measuring oxygen consumption rate (OCR), as a surrogate for viability, in freshly explanted TEGs after one week's residence subcutaneously (**Figure 1**). The results of OCR measurements (**Figures 4A–C**) supported the trend derived from the mathematical model, that viability decreases with increasing islet density, but the experimental observations indicated a more pronounced drop in viability at modest densities (500 IE/cm^2) and a more profound loss of viability at high islet densities (>2,000 IE/cm^2) than predicted (**Figures 3E,F**). Histologic examination was confirmatory; at a density of 4,000 IE/cm^2 (**Figure 4E**) compared to 500 IE/cm^2 (**Figure 4D**), far fewer cells stained positive for insulin; importantly, staining for caspase-3 indicated that many of the remaining islet cells were undergoing apoptosis. Although the images documented apoptosis, it must be assumed that necrosis had also occurred; several reports have noted that the two processes are often coincident, perhaps sequential (137–139). However, whether both apoptosis and necrosis are both primarily the consequence of hypoxia alone remains to be determined.

Our data and conclusions should not be taken as a blanket condemnation of this technology. Transplanting cells inside a TEG offers essential advantages (68, 70, 140, 141): it localizes the graft within the device, the cells are therefore more amenable to *in vivo* assessments and, if need be, can be retrieved. Previous efforts (142) to develop a tissue-engineered islet graft (or bioartificial pancreas) have struggled to achieve clinical translation (58, 61, 63, 143–145), but with recent developments in stem cell and xenogeneic islet technologies (87, 146–155) and the promise of scalable alternative β-cell sources (142, 151, 156, 157), there is a renewed interest in—and progress toward—developing a functional insulin-producing, cell-containing TEG for diabetes treatment (87, 158–161).

Previously published reports described the challenges of oxygenation for TEGs, especially in scenarios which require high cell-densities to achieve the therapeutic objective with a device of practical size (50, 55, 75, 162). The sham TEG measurements of available oxygen *in vivo* suggest that the subcutaneous space is profoundly hypoxic, with an average available PO2 of 12 (SEM 5) mmHg [and only 6.8 (SEM 10) mmHg in the peritoneal space].

These trends in oxygen levels are not statistically significant, but they are consistent with the pathophysiologic processes that follow a surgical insult and the implantation of foreign materials. TEGs implanted in the peritoneum had a similar PO2 trend and a similar hypoxic environment as subcutaneous TEGs during the 29-day period of observation (**Supplementary Information Figure S1**). The histological findings from explanted sham TEGs support this interpretation of the dynamic PO2 changes *in vivo* (**Supplemental Information Figure S2**). By 29 days, the surrounding tissue had developed a moderate amount of neovascularization; in comparison, only mild fibrosis and foreign body reaction were identified. These findings are consistent with previous reports using similar TEGs (75, 99, 103); fibrosis and foreign body reactions are not unexpected with these materials but can be effectively mitigated with induction of

neovascularization aided by the proper selection of materials and membrane microarchitecture (125, 163–165). It should be emphasized that neovascularization of TEGs having vascularizing external membranes is – in fact – a rapid process. Padera and Colton (164) have carefully documented the time course of vascularization of a suitable membrane: vascularity at the interface "increased up to 10 days and remained at this level even at 329 days post-implantation". Similar observations have been reported by others (88, 165, 166). Investigations of pro-angiogenic factors and other approaches to accelerate vascularization have recently been reviewed (167).

In summary, these results suggest that without oxygen supplementation, thin devices with high oxygen permeability are required to maintain viability of encapsulated tissues; even then, to ensure adequate islet function, only low islet densities can be loaded. To accommodate TEGs with low islet densities (≤500 IE/cm^2), very large implants would be required to achieve the surface area needed for oxygenation; a device of the required size would be impractical for implantation in humans (57). In addition to the hypoxic stress that encapsulated islets face within these TEGs, there are other *in vivo* considerations that may further decrease or limit the viability and function of such grafts. Although these considerations are beyond the scope of this work, they may help explain the greater viability loss observed in our experimental measurements using OCR in comparison to the model results. Oxygenation is especially challenging when using high cell densities, which create significant oxygen transport limitations within the graft (50). These challenges are recognized in recent reviews (50, 55, 128). Our results confirm a critical need for improved oxygenation in macroencapsulated TEGs to support the high-cell densities needed for therapeutic applications. Many engineered tissues for the treatment of human disease will require developing complex tissues with high (near native) cell densities to provide therapeutic benefit. Oxygenation is a critical challenge facing the field of tissue engineering and especially for encapsulation approaches that do not allow complete re-vascularization of tissues.

Data availability statement

The original contributions presented in the study are included in the article; further inquiries can be directed to the corresponding author.

Ethics statement

All animal research was performed with the approval of and in accordance with guidelines of the University of Minnesota and the University of Arizona Institutional Animal Care and Use Committees (IACUC). Procurement of human islets was approved and overseen by the University of California Institutional Review Board and informed consent was obtained for all donors. Ethical approval was not required for the studies on humans in accordance with the local legislation and institutional requirements because only commercially available established cell lines were used. The animal study was approved by University of Minnesota and the University of Arizona Institutional Animal Care and Use Committees (IACUC). The study was conducted in accordance with the local legislation and institutional requirements.

Author contributions

SE: Conceptualization, Data curation, Investigation, Writing – original draft, Writing – review & editing. LS: Conceptualization, Data curation, Investigation, Writing – original draft. BW: Writing – review & editing, Conceptualization, Data curation, Formal Analysis, Investigation, Methodology, Supervision, Visualization, Writing – original draft. TS: Conceptualization, Investigation, Writing – original draft. AS: Conceptualization, Methodology, Formal Analysis, Visualization, Writing – review & editing. TO: Conceptualization, Writing – original draft, Investigation. EA: Conceptualization, Data curation, Investigation, Writing – original draft. MF: Conceptualization, Writing – original draft. MLG: Conceptualization, Writing – original draft, Investigation. JJ: Investigation, Writing – original draft. LE: Writing – original draft, Data curation. MG: Data curation, Investigation, Writing – original draft, Writing – review & editing. CP: Writing – review & editing. KP: Conceptualization, Writing – original draft, Writing – review & editing.

Funding

The author(s) declare financial support was received for the research, authorship, and/or publication of this article.

JDRF Grants: JDRF 5-2013-141, 3-SRA-2015-40-Q-R. NIH Grants: P41 EB015894, S10 RR025031, P30 DK063720, P30 CA023074, 1DP3DK106933-01. Additional funding was provided by the Minnesota Lions Diabetes Foundation, the Schott Foundation, The Carol Olson Memorial Fund, and the Richard M. Schulze Family Foundation.

Acknowledgments

The authors dedicate this report to our co-author, Meri T. Firpo, who tragically passed prematurely before submission of the manuscript. Human islets were provided by the University of California, San Francisco, Islet and Cellular Production Facility which is supported by the Diabetes Endocrinology Research Center grant (NIH P30 DK063720). Histological samples for sham devices were processed by the Comparative Pathology Shared Resource (CPC) at the University of Minnesota. Immunohistochemical images of devices containing human islets were generated by the Tissue Acquisition and Cellular/Molecular Analysis Shared Service (TACMASR Core) which is supported by the University of Arizona Cancer Center Support grant (NIH P30 CA023074). The authors wish to acknowledge Chan A. Ion and Jennifer Kitzmann-Miner for their work in preparing graphic materials.

Conflict of interest

KP is the co-founder and CEO of Procyon Technologies, LLC, a startup company focused on the development of oxygenated cell encapsulation devices. BW, who was a graduate student at the time of this study, is now employed by Sylvatica Biotech Inc.

The remaining authors declare that the research was conducted in the absence of any commercial or financial relationships that could be construed as a potential conflict of interest.

The author MG declared that he was an editorial board member of Frontiers, at the time of submission. This had no impact on the peer review process and the final decision.

Publisher's note

Supplementary material

The Supplementary Material for this article can be found online at: https://www.frontiersin.org/articles/10.3389/frtra.2023.1257029/full#supplementary-material

References

1. Basile G, Qadir MMF, Mauvais-Jarvis F, Vetere A, Shoba V, Modell AE, et al. Emerging diabetes therapies: bringing back the β-cells. *Mol Metab*. (2022) 60:101477. doi: 10.1016/j.molmet.2022.101477

2. Hatipoglu BA, Blanchette J. Islet cell therapy and stem cell therapy for type 1 diabetes: there will always be a hope. *Endocrinol Metab Clin North Am*. (2023) 52 (1):187–93. doi: 10.1016/j.ecl.2022.07.001

3. Rickels MR, Robertson RP. Pancreatic islet transplantation in humans: recent progress and future directions. *Endocr Rev*. (2019) 40(2):631–68. doi: 10.1210/er.2018-00154

4. Oliveira SM R, Rebocho A, Ahmadpour E, Nissapatorn V, de Lourdes Pereira M. Type 1 diabetes Mellitus: a review on advances and challenges in creating insulin producing devices. *Micromachines (Basel)*. (2023) 14(1):151–80. doi: 10.3390/mi14010151

5. Shapiro AM, Pokrywczynska M, Ricordi C. Clinical pancreatic islet transplantation. *Nat Rev Endocrinol*. (2017) 13(5):268–77. doi: 10.1038/nrendo.2016.178

6. Aguayo-Mazzucato C, Bonner-Weir S. Stem cell therapy for type 1 diabetes mellitus. *Nat Rev Endocrinol*. (2010) 6(3):139–48. doi: 10.1038/nrendo.2009.274

7. Jiang H, Jiang FX. Human pluripotent stem cell-derived β cells: truly immature islet β cells for type 1 diabetes therapy? *World J Stem Cells*. (2023) 15(4):182–95. doi: 10.4252/wjsc.v15.i4.182

8. Marfil-Garza BA, Polishevska K, Pepper AR, Korbutt GS. Current state and evidence of cellular encapsulation strategies in type 1 diabetes. *Compr Physiol*. (2020) 10(3):839–78. doi: 10.1002/cphy.c190033

9. Stanekzai J, Isenovic ER, Mousa SA. Treatment options for diabetes: potential role of stem cells. *Diabetes Res Clin Pract*. (2012) 98(3):361–8. doi: 10.1016/j.diabres.2012.09.010

10. Hering BJ, Kandaswamy R, Ansite JD, Eckman PM, Nakano M, Sawada T, et al. Single-donor, marginal-dose islet transplantation in patients with type 1 diabetes. *JAMA*. (2005) 293(7):830–5. doi: 10.1001/jama.293.7.830

11. Jin SM, Kim KW. Is islet transplantation a realistic approach to curing diabetes? *Korean J Intern Med*. (2017) 32(1):62–6. doi: 10.3904/kjim.2016.224

12. Shapiro AM. State of the art of clinical islet transplantation and novel protocols of immunosuppression. *Curr Diab Rep*. (2011) 11(5):345–54. doi: 10.1007/s11892-011-0217-8

13. Toso C, Baertschiger R, Morel P, Bosco D, Armanet M, Wojtusciszyn A, et al. Sequential kidney/islet transplantation: efficacy and safety assessment of a steroid-free immunosuppression protocol. *Am J Transplant*. (2006) 6(5 Pt 1):1049–58. doi: 10.1111/j.1600-6143.2006.01303.x

14. Barton FB, Rickels MR, Alejandro R, Hering BJ, Wease S, Naziruddin B, et al. Improvement in outcomes of clinical islet transplantation: 1999-2010. *Diabetes Care*. (2012) 35(7):1436–45. doi: 10.2337/dc12-0063

15. Bellin MD, Barton FB, Heitman A, Harmon JV, Kandaswamy R, Balamurugan AN, et al. Potent induction immunotherapy promotes long-term insulin independence after islet transplantation in type 1 diabetes. *Am J Transplant*. (2012) 12(6):1576–83. doi: 10.1111/j.1600-6143.2011.03977.x

16. Bellin MD, Kandaswamy R, Parkey J, Zhang HJ, Liu B, Ihm SH, et al. Prolonged insulin independence after islet allotransplants in recipients with type 1 diabetes. *Am J Transplant*. (2008) 8(11):2463–70. doi: 10.1111/j.1600-6143.2008.02404.x

17. Froud T, Ricordi C, Baidal DA, Hafiz MM, Ponte G, Cure P, et al. Islet transplantation in type 1 diabetes mellitus using cultured islets and steroid-free immunosuppression: Miami experience. *Am J Transplant*. (2005) 5(8):2037–46. doi: 10.1111/j.1600-6143.2005.00957.x

18. Group CR. 2007 Update on allogeneic islet transplantation from the collaborative islet transplant registry (CITR). *Cell Transplant*. (2009) 18(7):753–67. doi: 10.3727/096368909X470874

19. Ryan EA, Paty BW, Senior PA, Bigam D, Alfadhli E, Kneteman NM, et al. Five-year follow-up after clinical islet transplantation. *Diabetes*. (2005) 54(7):2060–9. doi: 10.2337/diabetes.54.7.2060

20. Bergman ZR, Robbins AJ, Alwan FS, Bellin MD, Kirchner VA, Pruett TL, et al. Perioperative coagulation changes in total pancreatectomy and islet autotransplantation. *Pancreas*. (2022) 51(6):671–7. doi: 10.1097/MPA.0000000000002085

21. Moberg L, Johansson H, Lukinius A, Berne C, Foss A, Källen R, et al. Production of tissue factor by pancreatic islet cells as a trigger of detrimental thrombotic reactions in clinical islet transplantation. *Lancet*. (2002) 360(9350):2039–45. doi: 10.1016/S0140-6736(02)12020-4

22. Parks L, Routt M. Total pancreatectomy with islet cell transplantation for the treatment of pancreatic cancer. *Clin J Oncol Nurs*. (2015) 19(4):479–81. doi: 10.1188/15.CJON.479-481

23. Teramura Y, Iwata H. Islets surface modification prevents blood-mediated inflammatory responses. *Bioconjug Chem*. (2008) 19(7):1389–95. doi: 10.1021/bc800064t

24. Huurman VA, Hilbrands R, Pinkse GG, Gillard P, Duinkerken G, van de Linde P, et al. Cellular islet autoimmunity associates with clinical outcome of islet cell transplantation. *PLoS One*. (2008) 3(6):e2435. doi: 10.1371/journal.pone.0002435

25. Desai NM, Goss JA, Deng S, Wolf BA, Markmann E, Palanjian M, et al. Elevated portal vein drug levels of sirolimus and tacrolimus in islet transplant recipients: local immunosuppression or islet toxicity? *Transplantation*. (2003) 76(11):1623–5. doi: 10.1097/01.TP.0000081043.23751.81

26. Huh KH, Cho Y, Kim BS, Do JH, Park YJ, Joo DJ, et al. The role of thioredoxin 1 in the mycophenolic acid-induced apoptosis of insulin-producing cells. *Cell Death Dis*. (2013) 4(7):e721. doi: 10.1038/cddis.2013.247

27. Kloster-Jensen K, Sahraoui A, Vethe NT, Korsgren O, Bergan S, Foss A, et al. Treatment with tacrolimus and sirolimus reveals no additional adverse effects on human islets in vitro compared to each drug alone but they are reduced by adding glucocorticoids. *J Diabetes Res*. (2016) 2016:4196460. doi: 10.1155/2016/4196460

28. Laugharne M, Cross S, Richards S, Dawson C, Ilchyshyn L, Saleem M, et al. Sirolimus toxicity and vascular endothelial growth factor release from islet and renal cell lines. *Transplantation*. (2007) 83(12):1635–8. doi: 10.1097/01.tp.0000266555.06635.bf

29. Paty BW, Harmon JS, Marsh CL, Robertson RP. Inhibitory effects of immunosuppressive drugs on insulin secretion from HIT-T15 cells and wistar rat islets. *Transplantation*. (2002) 73(3):353–7. doi: 10.1097/00007890-200202150-00007

30. Piao SG, Lim SW, Doh KC, Jin L, Heo SB, Zheng YF, et al. Combined treatment of tacrolimus and everolimus increases oxidative stress by pharmacological interactions. *Transplantation*. (2014) 98(1):22–8. doi: 10.1097/TP.0000000000000146

31. Prud'homme GJ, Glinka Y, Hasilo C, Paraskevas S, Li X, Wang Q. GABA protects human islet cells against the deleterious effects of immunosuppressive drugs and exerts immunoinhibitory effects alone. *Transplantation*. (2013) 96 (7):616–23. doi: 10.1097/TP.0b013e31829c24be

32. Rodriguez-Rodriguez AE, Donate-Correa J, Rovira J, Cuesto G, Luis-Ravelo D, Fernandes MX, et al. Inhibition of the mTOR pathway: a new mechanism of β cell toxicity induced by tacrolimus. *Am J Transplant*. (2019) 19(12):3240–9. doi: 10.1111/ajt.15483

33. Triñanes J, Rodriguez-Rodriguez AE, Brito-Casillas Y, Wagner A, De Vries APJ, Cuesto G, et al. Deciphering tacrolimus-induced toxicity in pancreatic β cells. *Am J Transplant*. (2017) 17(11):2829–40. doi: 10.1111/ajt.14323

34. Carlsson PO, Palm F, Mattsson G. Low revascularization of experimentally transplanted human pancreatic islets. *J Clin Endocrinol Metab*. (2002) 87 (12):5418–23. doi: 10.1210/jc.2002-020728

35. Hughes SJ, Davies SE, Powis SH, Press M. Hyperoxia improves the survival of intraportally transplanted syngeneic pancreatic islets. *Transplantation*. (2003) 75 (12):1954–9. doi: 10.1097/01.TP.0000066805.39716.23

36. Lau J, Carlsson PO. Low revascularization of human islets when experimentally transplanted into the liver. *Transplantation*. (2009) 87(3):322–5. doi: 10.1097/TP.0b013e3181943b3d

37. Lau J, Henriksnäs J, Svensson J, Carlsson PO. Oxygenation of islets and its role in transplantation. *Curr Opin Organ Transplant*. (2009) 14(6):688–93. doi: 10.1097/MOT.0b013e32833239ff

38. Liljebäck H, Grapensparr L, Olerud J, Carlsson PO. Extensive loss of islet mass beyond the first day after intraportal human islet transplantation in a mouse model. *Cell Transplant*. (2016) 25(3):481–9. doi: 10.3727/096368915X688902

39. Mattsson G, Jansson L, Carlsson PO. Decreased vascular density in mouse pancreatic islets after transplantation. *Diabetes*. (2002) 51(5):1362–6. doi: 10.2337/diabetes.51.5.1362

40. Olsson R, Olerud J, Pettersson U, Carlsson PO. Increased numbers of low-oxygenated pancreatic islets after intraportal islet transplantation. *Diabetes*. (2011) 60(9):2350–3. doi: 10.2337/db09-0490

41. Sakata N, Chan NK, Ostrowski RP, Chrisler J, Hayes P, Kim S, et al. Hyperbaric oxygen therapy improves early posttransplant islet function. *Pediatr Diabetes*. (2010) 11(7):471–8. doi: 10.1111/j.1399-5448.2009.00629.x

42. Smith KE, Kelly AC, Min CG, Weber CS, McCarthy FM, Steyn LV, et al. Acute ischemia induced by high-density culture increases cytokine expression and diminishes the function and viability of highly purified human islets of langerhans. *Transplantation*. (2017) 101(11):2705–12. doi: 10.1097/TP.0000000000001714

43. Suszynski TM, Avgoustiniatos ES, Papas KK. Intraportal islet oxygenation. *J Diabetes Sci Technol*. (2014) 8(3):575–80. doi: 10.1177/1932296814525827

44. Suszynski TM, Avgoustiniatos ES, Papas KK. Oxygenation of the intraportally transplanted pancreatic islet. *J Diabetes Res*. (2016) 2016:7625947. doi: 10.1155/2016/7625947

45. Chen X, Kaufman DB. Bioluminescent imaging of transplanted islets. *Methods Mol Biol*. (2009) 574:75–85. doi: 10.1007/978-1-60327-321-3_7

46. Vantyghem MC, Beron A, Pattou F, Engelse MA, Velikyan I, Eriksson O, et al. Monitoring β-cell survival after intrahepatic islet transplantation using dynamic exendin PET imaging: a proof-of-concept study in individuals with type 1 diabetes. *Diabetes*. (2023) 72(7):898–907. doi: 10.2337/db22-0884

47. Liljebäck H, Espes D, Carlsson PO. Unsurpassed intrahepatic islet engraftment - the quest for new sites for Beta cell replacement. *Cell Med*. (2019) 11:2155179019857662. doi: 10.1177/2155179019857662

48. Medarova Z, Moore A. MRI as a tool to monitor islet transplantation. *Nat Rev Endocrinol*. (2009) 5(8):444–52. doi: 10.1038/nrendo.2009.130

49. Wang P, Schuetz C, Vallabhajosyula P, Medarova Z, Tena A, Wei L, et al. Monitoring of allogeneic islet grafts in nonhuman primates using MRI. *Transplantation*. (2015) 99(8):1574–81. doi: 10.1097/TP.0000000000000682

50. Colton CK. Oxygen supply to encapsulated therapeutic cells. *Adv Drug Deliv Rev*. (2014) 67-68:93–110. doi: 10.1016/j.addr.2014.02.007

51. Ludwig B, Reichel A, Steffen A, Zimerman B, Schally AV, Block NL, et al. Transplantation of human islets without immunosuppression. *Proc Natl Acad Sci U S A*. (2013) 110(47):19054–8. doi: 10.1073/pnas.1317561110

52. Ludwig B, Zimerman B, Steffen A, Yavriants K, Azarov D, Reichel A, et al. A novel device for islet transplantation providing immune protection and oxygen supply. *Horm Metab Res*. (2010) 42(13):918–22. doi: 10.1055/s-0030-1267916

53. Wang LH, Ernst AU, Flanders JA, Liu W, Wang X, Datta AK, et al. An inverse-breathing encapsulation system for cell delivery. *Sci Adv*. (2021) 7(20). doi: 10.1126/sciadv.abd5835

54. Yang HK, Ham DS, Park HS, Rhee M, You YH, Kim MJ, et al. Long-term efficacy and biocompatibility of encapsulated islet transplantation with chitosan-coated alginate capsules in mice and canine models of diabetes. *Transplantation*. (2016) 100(2):334–43. doi: 10.1097/TP.0000000000000927

55. Yang HK, Yoon KH. Current status of encapsulated islet transplantation. *J Diabetes Complications*. (2015) 29(5):737–43. doi: 10.1016/j.jdiacomp.2015.03.017

56. Kuwabara R, Hu S, Smink AM, Orive G, Lakey JRT, de Vos P. Applying immunomodulation to promote longevity of immunoisolated pancreatic islet grafts. *Tissue Eng Part B Rev*. (2022) 28(1):129–40. doi: 10.1089/ten.teb.2020.0326

57. Papas KK, Avgoustiniatos ES, Suszynski TM. Effect of oxygen supply on the size of implantable islet-containing encapsulation devices. *Panminerva Med*. (2016) 58 (1):72–7. PMID: 26837777.

58. Papas KK, Long RC Jr., Sambanis A, Constantinidis I. Development of a bioartificial pancreas: II. Effects of oxygen on long-term entrapped betaTC3 cell cultures. *Biotechnol Bioeng*. (1999) 66(4):231–7. doi: 10.1002/(SICI)1097-0290(1999)66:4<231::AID-BIT4>3.0.CO;2-U

59. Rafael E, Wernerson A, Arner P, Tibell A. In vivo studies on insulin permeability of an immunoisolation device intended for islet transplantation using the microdialysis technique. *Eur Surg Res*. (1999) 31(3):249–58. doi: 10.1159/000008700

60. Rafael E, Wernerson A, Arner P, Wu GS, Tibell A. In vivo evaluation of glucose permeability of an immunoisolation device intended for islet transplantation: a novel application of the microdialysis technique. *Cell Transplant*. (1999) 8(3):317–26. doi: 10.1177/096368979900800302

61. Sambanis A, Papas KK, Flanders PC, Long RC Jr., Kang H, Constantinidis I. Towards the development of a bioartificial pancreas: immunoisolation and NMR monitoring of mouse insulinomas. *Cytotechnology*. (1994) 15(1-3):351–63. doi: 10.1007/BF00762410

62. Samojlik MM, Stabler CL. Designing biomaterials for the modulation of allogeneic and autoimmune responses to cellular implants in type 1 diabetes. *Acta Biomater*. (2021) 133:87–101. doi: 10.1016/j.actbio.2021.05.039

63. Tziampazis E, Sambanis A. Tissue engineering of a bioartificial pancreas: modeling the cell environment and device function. *Biotechnol Prog*. (1995) 11 (2):115–26. doi: 10.1021/bp00032a001

64. Anazawa T, Balamurugan AN, Bellin M, Zhang HJ, Matsumoto S, Yonekawa Y, et al. Human islet isolation for autologous transplantation: comparison of yield and function using SERVA/nordmark versus roche enzymes. *Am J Transplant*. (2009) 9 (10):2383–91. doi: 10.1111/j.1600-6143.2009.02765.x

65. Bampton TJ, Holmes-Walker DJ, Drogemuller CJ, Radford T, Anderson P, Etherton C, et al. Australian experience with total pancreatectomy with islet autotransplantation to treat chronic pancreatitis. *ANZ J Surg*. (2021) 91(12):2663–8. doi: 10.1111/ans.16853

66. Turner KM, Delman AM, Donovan EC, Brunner J, Wahab SA, Dai Y, et al. Total pancreatectomy and islet cell autotransplantation: a 10-year update on outcomes and assessment of long-term durability. *HPB (Oxford)*. (2022) 24(11):2013–21. doi: 10.1016/j.hpb.2022.07.001

67. Ernst AU, Wang LH, Worland SC, Marfil-Garza BA, Wang X, Liu W, et al. A predictive computational platform for optimizing the design of bioartificial pancreas devices. *Nat Commun*. (2022) 13(1):6031. doi: 10.1038/s41467-022-33760-5

68. Iwata H, Arima Y, Tsutsui Y. Design of bioartificial pancreases from the standpoint of oxygen supply. *Artif Organs*. (2018) 42(8):E168–E85. doi: 10.1111/aor.13106

69. Fernandez SA, Champion KS, Danielczak L, Gasparrini M, Paraskevas S, Leask RL, et al. Engineering vascularized islet macroencapsulation devices: an in vitro platform to study oxygen transport in perfused immobilized pancreatic beta cell cultures. *Front Bioeng Biotechnol*. (2022) 10:884071. doi: 10.3389/fbioe.2022.884071

70. Wang X, Maxwell KG, Wang K, Bowers DT, Flanders JA, Liu W, et al. A nanofibrous encapsulation device for safe delivery of insulin-producing cells to treat type 1 diabetes. *Sci Transl Med*. (2021) 13(596):eabb4601. doi: 10.1126/scitranslmed.abb4601

71. Dufrane D, Steenberghe M, Goebbels RM, Saliez A, Guiot Y, Gianello P. The influence of implantation site on the biocompatibility and survival of alginate encapsulated pig islets in rats. *Biomaterials*. (2006) 27(17):3201–8. doi: 10.1016/j.biomaterials.2006.01.028

72. Lund T, Korsgren O, Aursnes IA, Scholz H, Foss A. Sustained reversal of diabetes following islet transplantation to striated musculature in the rat. *J Surg Res*. (2010) 160(1):145–54. doi: 10.1016/j.jss.2008.11.009

73. Windt DJ VD, Echeverri GJ, Ijzermans JNM, Cooper DKC. The choice of anatomical site for islet transplantation. *Cell Transplant*. (2008) 17(9):1005–14. doi: 10.3727/096368908786991515

74. Cantarelli E, Piemonti L. Alternative transplantation sites for pancreatic islet grafts. *Curr Diab Rep*. (2011) 11(5):364–74. doi: 10.1007/s11892-011-0216-9

75. Chhabra P, Brayman KL. Overcoming barriers in clinical islet transplantation: current limitations and future prospects. *Curr Probl Surg*. (2014) 51(2):49–86. doi: 10.1067/j.cpsurg.2013.10.002

76. Merani S, Toso C, Emamaullee J, Shapiro AM. Optimal implantation site for pancreatic islet transplantation. *Br J Surg*. (2008) 95(12):1449–61. doi: 10.1002/bjs.6391

77. Rajab A. Islet transplantation: alternative sites. *Curr Diab Rep*. (2010) 10 (5):332–7. doi: 10.1007/s11892-010-0130-6

78. Arifin DR, Valdeig S, Anders RA, Bulte JW, Weiss CR. Magnetoencapsulated human islets xenotransplanted into swine: a comparison of different transplantation sites. *Xenotransplantation*. (2016) 23(3):211–21. doi: 10.1111/xen.12235

79. Coronel MM, Liang JP, Li Y, Stabler CL. Oxygen generating biomaterial improves the function and efficacy of beta cells within a macroencapsulation device. *Biomaterials*. (2019) 210:1–11. doi: 10.1016/j.biomaterials.2019.04.017

80. Komatsu H, Cook CA, Gonzalez N, Medrano L, Salgado M, Sui F, et al. Oxygen transporter for the hypoxic transplantation site. *Biofabrication*. (2018) 11(1):015011. doi: 10.1088/1758-5090/aaf2f0

81. Mitchelson F, Safley SA, Gordon K, Weber CJ, Sambanis A. Peritoneal dissolved oxygen and function of encapsulated adult porcine islets transplanted in streptozotocin diabetic mice. *Xenotransplantation*. (2021) 28(3):e12673. doi: 10.1111/xen.12673

82. Razavi M, Primavera R, Kevadiya BD, Wang J, Buchwald P, Thakor AS. A collagen based cryogel bioscaffold that generates oxygen for islet transplantation. *Adv Funct Mater*. (2020) 30(15). doi: 10.1002/adfm.201902463

83. Skrzypek K, Groot Nibbelink M, Liefers-Visser J, Smink AM, Stoimenou E, Engelse MA, et al. A high cell-bearing capacity multibore hollow fiber device for macroencapsulation of islets of langerhans. *Macromol Biosci*. (2020) 20(8):e2000021. doi: 10.1002/mabi.202000021

84. Einstein SA, Weegman BP, Firpo MT, Papas KK, Garwood M. Development and validation of noninvasive magnetic resonance relaxometry for the in vivo assessment of tissue-engineered graft oxygenation. *Tissue Eng Part C Methods*. (2016) 22 (11):1009–17. doi: 10.1089/ten.tec.2016.0106

85. Suszynski TM, Avgoustiniatos ES, Stein SA, Falde EJ, Hammer BE, Papas KK. Assessment of tissue-engineered islet graft viability by fluorine magnetic resonance spectroscopy. *Transplant Proc*. (2011) 43(9):3221–5. doi: 10.1016/j.transproceed.2011.09.009

86. El-Halawani SM, Gabr MM, El-Far M, Zakaria MM, Khater SM, Refaie AF, et al. Subcutaneous transplantation of bone marrow derived stem cells in macroencapsulation device for treating diabetic rats; clinically transplantable site. *Heliyon*. (2020) 6(5):e03914. doi: 10.1016/j.heliyon.2020.e03914

87. Lee SH, Hao E, Savinov AY, Geron I, Strongin AY, Itkin-Ansari P. Human beta-cell precursors mature into functional insulin-producing cells in an immunoisolation device: implications for diabetes cell therapies. *Transplantation*. (2009) 87(7):983–91. doi: 10.1097/TP.0b013e31819c86ea

88. Rafael E, Wu GS, Hultenby K, Tibell A, Wernerson A. Improved survival of macroencapsulated islets of langerhans by preimplantation of the immunoisolating device: a morphometric study. *Cell Transplant*. (2003) 12(4):407–12. doi: 10.3727/000000003108746957

89. Sorenby AK, Kumagai-Braesch M, Sharma A, Hultenby KR, Wernerson AM, Tibell AB. Preimplantation of an immunoprotective device can lower the curative dose of islets to that of free islet transplantation: studies in a rodent model. *Transplantation*. (2008) 86(2):364–6. doi: 10.1097/TP.0b013e31817efc78

90. Sweet IR, Yanay O, Waldron L, Gilbert M, Fuller JM, Tupling T, et al. Treatment of diabetic rats with encapsulated islets. *J Cell Mol Med*. (2008) 12(6b):2644–50. doi: 10.1111/j.1582-4934.2008.00322.x

91. Tibell A, Rafael E, Wennberg L, Nordenstrom J, Bergstrom M, Geller RL, et al. Survival of macroencapsulated allogeneic parathyroid tissue one year after transplantation in nonimmunosuppressed humans. *Cell Transplant*. (2001) 10 (7):591–9. doi: 10.3727/000000001783986404

92. Trivedi N, Steil GM, Colton CK, Bonner-Weir S, Weir GC. Improved vascularization of planar membrane diffusion devices following continuous infusion of vascular endothelial growth factor. *Cell Transplant*. (2000) 9(1):115–24. doi: 10.1177/096368970000900114

93. Boettler T, Schneider D, Cheng Y, Kadoya K, Brandon EP, Martinson L, et al. Pancreatic tissue transplanted in TheraCyte encapsulation devices is protected and prevents hyperglycemia in a mouse model of immune-mediated diabetes. *Cell Transplant*. (2016) 25(3):609–14. doi: 10.3727/096368915X688939

94. Bruin JE, Rezania A, Xu J, Narayan K, Fox JK, O'Neil JJ, et al. Maturation and function of human embryonic stem cell-derived pancreatic progenitors in macroencapsulation devices following transplant into mice. *Diabetologia*. (2013) 56 (9):1987–98. doi: 10.1007/s00125-013-2955-4

95. David A, Day J, Shikanov A. Immunoisolation to prevent tissue graft rejection: current knowledge and future use. *Exp Biol Med (Maywood)*. (2016) 241(9):955–61. doi: 10.1177/1535370216647129

96. Kompa AR, Greening DW, Kong AM, McMillan PJ, Fang H, Saxena R, et al. Sustained subcutaneous delivery of secretome of human cardiac stem cells promotes cardiac repair following myocardial infarction. *Cardiovasc Res*. (2021) 117 (3):918–29. doi: 10.1093/cvr/cvaa088

97. Kumagai-Braesch M, Jacobson S, Mori H, Jia X, Takahashi T, Wernerson A, et al. The TheraCyte^{TM} device protects against islet allograft rejection in immunized hosts. *Cell Transplant*. (2013) 22(7):1137–46. doi: 10.3727/096368912X657486

98. Tarantal AF, Lee CC, Itkin-Ansari P. Real-time bioluminescence imaging of macroencapsulated fibroblasts reveals allograft protection in rhesus monkeys (Macaca mulatta). *Transplantation*. (2009) 88(1):38–41. doi: 10.1097/TP.0b013e3181a9ee6c

99. Colton CK. Chapter 28 - challenges in the development of immunoisolation devices. In: Robert L, Robert L, Joseph V, editors. *Principles of tissue engineering (fourth edition)*. 4 edn edn. Boston: Academic Press (2014). p. 543–62.

100. Barkai U, Weir GC, Colton CK, Ludwig B, Bornstein SR, Brendel MD, et al. Enhanced oxygen supply improves islet viability in a new bioartificial pancreas. *Cell Transplant*. (2013) 22(8):1463–76. doi: 10.3727/096368912X657341

101. Avgoustiniatos ES, Wu H, Colton CK. Engineering challenges in immunoisolation device development. In: *Principles of tissue engineering*. San Diego: Academic Press (2000). p. 331–50. doi: 10.1016/B978-012436630-5/50031-3

102. Colton CK. Implantable biohybrid artificial organs. *Cell Transplant*. (1995) 4 (4):415–36. doi: 10.1177/096368979500400413

103. Avgoustiniatos ES, Colton CK. Effect of external oxygen mass transfer resistances on viability of immunoisolated tissue. *Ann N Y Acad Sci*. (1997) 831:145–67. doi: 10.1111/j.1749-6632.1997.tb52192.x

104. Papas KK, Colton CK, Qipo A, Wu H, Nelson RA, Hering BJ, et al. Prediction of marginal mass required for successful islet transplantation. *J Invest Surg*. (2010) 23 (1):28–34. doi: 10.3109/08941930903410825

105. Carlsson PO, Palm F, Andersson A, Liss P. Markedly decreased oxygen tension in transplanted rat pancreatic islets irrespective of the implantation site. *Diabetes*. (2001) 50(3):489–95. doi: 10.2337/diabetes.50.3.489

106. Goh F, Sambanis A. In vivo noninvasive monitoring of dissolved oxygen concentration within an implanted tissue-engineered pancreatic construct. *Tissue Eng Part C Methods*. (2011) 17(9):887–94. doi: 10.1089/ten.tec.2011.0098

107. Gross JD, Long RC Jr., Constantinidis I, Sambanis A. Monitoring of dissolved oxygen and cellular bioenergetics within a pancreatic substitute. *Biotechnol Bioeng*. (2007) 98(1):261–70. doi: 10.1002/bit.21421

108. Intaglietta M, Johnson PC, Winslow RM. Microvascular and tissue oxygen distribution. *Cardiovasc Res*. (1996) 32(4):632–43. doi: 10.1016/S0008-6363(96)00110-1

109. Lutz J, Noth U, Morrissey SP, Adolf H, Deichmann R, Haase A. Measurement of oxygen tensions in the abdominal cavity and in the skeletal muscle using 19F-MRI of neat PFC droplets. *Adv Exp Med Biol*. (1997) 428:569–72. doi: 10.1007/978-1-4615-5399-1_80

110. Noth U, Grohn P, Jork A, Zimmermann U, Haase A, Lutz J. 19F-MRI in vivo determination of the partial oxygen pressure in perfluorocarbon-loaded alginate capsules implanted into the peritoneal cavity and different tissues. *Magn Reson Med*. (1999) 42(6):1039–47. doi: 10.1002/(SICI)1522-2594(199912)42:6<1039::AID-MRM8>3.0.CO;2-N

111. Dionne KE, Colton CK, Yarmush ML. Effect of hypoxia on insulin secretion by isolated rat and canine islets of langerhans. *Diabetes*. (1993) 42(1):12–21. doi: 10.2337/diab.42.1.12

112. Kitzmann JP, Pepper AR, Gala-Lopez B, Pawlick R, Kin T, O'Gorman D, et al. Human islet viability and function is maintained during high-density shipment in silicone rubber membrane vessels. *Transplant Proc*. (2014) 46(6):1989–91. doi: 10.1016/j.transproceed.2014.06.002

113. Papas KK, Avgoustiniatos ES, Tempelman LA, Weir GC, Colton CK, Pisania A, et al. High-density culture of human islets on top of silicone rubber membranes. *Transplant Proc*. (2005) 37(8):3412–4. doi: 10.1016/j.transproceed.2005.09.086

114. Papas KK, Colton CK, Nelson RA, Rozak PR, Avgoustiniatos ES, Scott WE 3rd, et al., Human islet oxygen consumption rate and DNA measurements predict diabetes reversal in nude mice. *Am J Transplant*. (2007) 7(3):707–13. doi: 10.1111/j.1600-6143.2006.01655.x

115. Pisania A, Papas KK, Powers DE, Rappel MJ, Omer A, Bonner-Weir S, et al. Enumeration of islets by nuclei counting and light microscopic analysis. *Lab Invest*. (2010) 90(11):1676–86. doi: 10.1038/labinvest.2010.125

116. Suszynski TM, Wildey GM, Falde EJ, Cline GW, Maynard KS, Ko N, et al. The ATP/DNA ratio is a better indicator of islet cell viability than the ADP/ATP ratio. *Transplant Proc*. (2008) 40(2):346–50. doi: 10.1016/j.transproceed.2008.01.061

117. Papas KK, Pisania A, Wu H, Weir GC, Colton CK. A stirred microchamber for oxygen consumption rate measurements with pancreatic islets. *Biotechnol Bioeng*. (2007) 98(5):1071–82. doi: 10.1002/bit.21486

118. Cole L, Anderson M, Antin PB, Limesand SW. One process for pancreatic beta-cell coalescence into islets involves an epithelial-mesenchymal transition. *J Endocrinol*. (2009) 203(1):19–31. doi: 10.1677/JOE-09-0072

119. Pedersen TO, Blois AL, Xue Y, Xing Z, Sun Y, Finne-Wistrand A, et al. Mesenchymal stem cells induce endothelial cell quiescence and promote capillary formation. *Stem Cell Res Ther*. (2014) 5(1):23. doi: 10.1186/scrt412

120. Tatarkiewicz K, Hollister-Lock J, Quickel RR, Colton CK, Bonner-Weir S, Weir GC. Reversal of hyperglycemia in mice after subcutaneous transplantation of macroencapsulated islets. *Transplantation*. (1999) 67(5):665–71. doi: 10.1097/00007890-199903150-00005

121. Vériter S, Aouassar N, Adnet PY, Paridaens MS, Stuckman C, Jordan B, et al. The impact of hyperglycemia and the presence of encapsulated islets on oxygenation within a bioartificial pancreas in the presence of mesenchymal stem cells in a diabetic wistar rat model. *Biomaterials*. (2011) 32(26):5945–56. doi: 10.1016/j.biomaterials.2011.02.061

122. Cottle L, Gan WJ, Gilroy I, Samra JS, Gill AJ, Loudovaris T, et al. Structural and functional polarisation of human pancreatic beta cells in islets from organ donors with and without type 2 diabetes. *Diabetologia*. (2021) 64(3):618–29. doi: 10.1007/s00125-020-05345-8

123. Chen W, Yung BC, Qian Z, Chen X. Improving long-term subcutaneous drug delivery by regulating material-bioenvironment interaction. *Adv Drug Deliv Rev*. (2018) 127:20–34. doi: 10.1016/j.addr.2018.01.016

124. Steyn LV, Drew D, Vlachos D, Huey B, Cocchi K, Price ND, et al. Accelerated absorption of regular insulin administered via a vascularizing permeable microchamber implanted subcutaneously in diabetic rattus norvegicus. *PLoS One*. (2023) 18(6):e0278794. doi: 10.1371/journal.pone.0278794

125. Brauker J, Martinson LA, Young SK, Johnson RC. Local inflammatory response around diffusion chambers containing xenografts. Nonspecific destruction of tissues and decreased local vascularization. *Transplantation*. (1996) 61(12):1671–7. doi: 10.1097/00007890-199606270-00002

126. Viswakarma N, Siddiqui E, Patel S, Hameed S, Schreiber W, Swartz HM, et al. In vivo partial oxygen pressure assessment in subcutaneous and intraperitoneal sites using imaging of solid oxygen probe. *Tissue Eng Part C Methods*. (2022) 28 (6):264–71. doi: 10.1089/ten.tec.2022.0061

127. Papas KK, Long RC Jr., Constantinidis I, Sambanis A. Effects of oxygen on metabolic and secretory activities of beta TC3 cells. *Biochim Biophys Acta*. (1996) 1291(2):163–6. doi: 10.1016/0304-4165(96)00062-1

128. Papas KK, De Leon H, Suszynski TM, Johnson RC. Oxygenation strategies for encapsulated islet and beta cell transplants. *Adv Drug Deliv Rev*. (2019) 139:139–56. doi: 10.1016/j.addr.2019.05.002

129. Whalen DW, Ding Z, Fournier RL. Method for measuring in vivo oxygen transport rates in a bioartificial organ. *Tissue Eng*. (1999) 5(2):81–9. doi: 10.1089/ten.1999.5.81

130. Caserto JS, Bowers DT, Shariati K, Ma M. Biomaterial applications in islet encapsulation and transplantation. *ACS Appl Bio Mater*. (2020) 3(12):8127–35. doi: 10.1021/acsabm.0c01235

131. McQuilling JP, Sittadjody S, Pendergraft S, Farney AC, Opara EC. Applications of particulate oxygen-generating substances (POGS) in the bioartificial pancreas. *Biomater Sci*. (2017) 5(12):2437–47. doi: 10.1039/C7BM00790F

132. An D, Wang LH, Ernst AU, Chiu A, Lu YC, Flanders JA, et al. An atmosphere-breathing refillable biphasic device for cell replacement therapy. *Adv Mater*. (2019) 31 (52):e1905135. doi: 10.1002/adma.201905135

133. Evron Y, Colton CK, Ludwig B, Weir GC, Zimermann B, Maimon S, et al. Long-term viability and function of transplanted islets macroencapsulated at high density are achieved by enhanced oxygen supply. *Sci Rep*. (2018) 8(1):6508. doi: 10.1038/s41598-018-23862-w

134. Tokito F, Shinohara M, Maruyama M, Inamura K, Nishikawa M, Sakai Y. High density culture of pancreatic islet-like 3D tissue organized in oxygen-permeable porous scaffolds with external oxygen supply. *J Biosci Bioeng*. (2021) 131(5):543–8. doi: 10.1016/j.jbiosc.2020.12.009

135. Accolla RP, Liang JP, Lansberry TR, Miravet IL, Loaisiga M, Sardi BL, et al. Engineering modular, oxygen-generating microbeads for the in situ mitigation of cellular hypoxia. *Adv Healthc Mater*. (2023) 12(19):e2300239. doi: 10.1002/adhm.202300239

136. Liang JP, Accolla RP, Soundirarajan M, Emerson A, Coronel MM, Stabler CL. Engineering a macroporous oxygen-generating scaffold for enhancing islet cell transplantation within an extrahepatic site. *Acta Biomater*. (2021) 130:268–80. doi: 10.1016/j.actbio.2021.05.028

137. de Groot M, Schuurs TA, Keizer PP, Fekken S, Leuvenink HG, van Schilfgaarde R. Response of encapsulated rat pancreatic islets to hypoxia. *Cell Transplant*. (2003) 12 (8):867–75. doi: 10.3727/000000003771000219

138. Giuliani M, Moritz W, Bodmer E, Dindo D, Kugelmeier P, Lehmann R, et al. Central necrosis in isolated hypoxic human pancreatic islets: evidence for postisolation ischemia. *Cell Transplant*. (2005) 14(1):67–76. doi: 10.3727/000000005783983287

139. Itoh T, Sugimoto K, Takita M, Shimoda M, Chujo D, SoRelle JA, et al. Low temperature condition prevents hypoxia-induced islet cell damage and HMGB1 release in a mouse model. *Cell Transplant*. (2012) 21(7):1361–70. doi: 10.3727/096368912X637514

140. Tomei AA, Villa C, Ricordi C. Development of an encapsulated stem cell-based therapy for diabetes. *Expert Opin Biol Ther*. (2015) 15(9):1321–36. doi: 10.1517/14712598.2015.1055242

141. Carlsson PO, Espes D, Sedigh A, Rotem A, Zimerman B, Grinberg H, et al. Transplantation of macroencapsulated human islets within the bioartificial pancreas *β*air to patients with type 1 diabetes mellitus. *Am J Transplant*. (2018) 18 (7):1735–44. doi: 10.1111/ajt.14642

142. Rood PP, Buhler LH, Bottino R, Trucco M, Cooper DK. Pig-to-nonhuman primate islet xenotransplantation: a review of current problems. *Cell Transplant*. (2006) 15(2):89–104. doi: 10.3727/000000006783982052

143. Grundfest-Broniatowski SF, Tellioglu G, Rosenthal KS, Kang J, Erdodi G, Yalcin B, et al. A new bioartificial pancreas utilizing amphiphilic membranes for the immunoisolation of porcine islets: a pilot study in the canine. *ASAIO J*. (2009) 55(4):400–5. doi: 10.1097/MAT.0b013e3181a8deba

144. Mikos AG, Papadaki MG, Kouvroukoglou S, Ishaug SL, Thomson RC. Mini-review: islet transplantation to create a bioartificial pancreas. *Biotechnol Bioeng*. (1994) 43(7):673–7. doi: 10.1002/bit.260430717

145. Papas KK, Long RC Jr., Sambanis A, Constantinidis I. Development of a bioartificial pancreas: I. Long-term propagation and basal and induced secretion from entrapped betaTC3 cell cultures. *Biotechnol Bioeng*. (1999) 66(4):219–30. doi: 10.1002/(SICI)1097-0290(1999)66:4<219::AID-BIT3>3.0.CO;2-B

146. Carvalho AM, Nunes R, Sarmento B. From pluripotent stem cells to bioengineered islets: a challenging journey to diabetes treatment. *Eur J Pharm Sci*. (2022) 172:106148. doi: 10.1016/j.ejps.2022.106148

147. Dinnyes A, Schnur A, Muenthaisong S, Bartenstein P, Burcez CT, Burton N, et al. Integration of nano- and biotechnology for beta-cell and islet transplantation in type-1 diabetes treatment. *Cell Prolif*. (2020) 53(5):e12785. doi: 10.1111/cpr.12785

148. Liu Y, Yang M, Cui Y, Yao Y, Liao M, Yuan H, et al. A novel prevascularized tissue-engineered chamber as a site for allogeneic and xenogeneic islet transplantation to establish a bioartificial pancreas. *PLoS One*. (2020) 15(12):e0234670. doi: 10.1371/journal.pone.0234670

149. Ludwig B, Ludwig S. Transplantable bioartificial pancreas devices: current status and future prospects. *Langenbecks Arch Surg*. (2015) 400(5):531–40. doi: 10.1007/s00423-015-1314-y

150. Orive G, Emerich D, Khademhosseini A, Matsumoto S, Hernández RM, Pedraz JL, et al. Engineering a clinically translatable bioartificial pancreas to treat type I diabetes. *Trends Biotechnol*. (2018) 36(4):445–56. doi: 10.1016/j.tibtech.2018.01.007

151. Aoki T, Hui H, Umehara Y, LiCalzi S, Demetriou AA, Rozga J, et al. Intrasplenic transplantation of encapsulated genetically engineered mouse insulinoma cells reverses streptozotocin-induced diabetes in rats. *Cell Transplant*. (2005) 14(6):411–21. doi: 10.3727/000000005783982990

152. Bose B, Katikireddy KR, Shenoy PS. Regenerative medicine for diabetes: differentiation of human pluripotent stem cells into functional beta-cells in vitro and their proposed journey to clinical translation. *Vitam Horm*. (2014) 95:223–48. doi: 10.1016/B978-0-12-800174-5.00009-0

153. Kroon E, Martinson LA, Kadoya K, Bang AG, Kelly OG, Eliazer S, et al. Pancreatic endoderm derived from human embryonic stem cells generates glucose-responsive insulin-secreting cells in vivo. *Nat Biotechnol*. (2008) 26(4):443–52. doi: 10.1038/nbt1393

154. Li W, Cavelti-Weder C, Zhang Y, Clement K, Donovan S, Gonzalez G, et al. Long-term persistence and development of induced pancreatic beta cells generated by lineage conversion of acinar cells. *Nat Biotechnol*. (2014) 32(12):1223–30. doi: 10.1038/nbt.3082

155. Li W, Nakanishi M, Zumsteg A, Shear M, Wright C, Melton DA, et al. In vivo reprogramming of pancreatic acinar cells to three islet endocrine subtypes. *Elife*. (2014) 3:e01846. doi: 10.7554/eLife.01846

156. Marchetti P, Finke EH, Gerasimidi-Vazeou A, Falqui L, Scharp DW, Lacy PE. Automated large-scale isolation, in vitro function and xenotransplantation of porcine islets of langerhans. *Transplantation*. (1991) 52(2):209–13. doi: 10.1097/00007890-199108000-00005

157. Simpson NE, Khokhlova N, Oca-Cossio JA, McFarlane SS, Simpson CP, Constantinidis I. Effects of growth regulation on conditionally-transformed alginate-entrapped insulin secreting cell lines in vitro. *Biomaterials*. (2005) 26(22):4633–41. doi: 10.1016/j.biomaterials.2004.11.054

158. Jeyagaran A, Lu CE, Zbinden A, Birkenfeld AL, Brucker SY, Layland SL. Type 1 diabetes and engineering enhanced islet transplantation. *Adv Drug Deliv Rev*. (2022) 189:114481. doi: 10.1016/j.addr.2022.114481

159. Nair GG, Tzanakakis ES, Hebrok M. Emerging routes to the generation of functional *β*-cells for diabetes mellitus cell therapy. *Nat Rev Endocrinol*. (2020) 16 (9):506–18. doi: 10.1038/s41574-020-0375-3

160. Siwakoti P, Rennie C, Huang Y, Li JJ, Tuch BE, McClements L, et al. Challenges with cell-based therapies for type 1 diabetes Mellitus. *Stem Cell Rev Rep*. (2023) 19 (3):601–24. doi: 10.1007/s12015-022-10482-1

161. Neumann M, Arnould T, Su BL. Encapsulation of stem-cell derived *β*-cells: a promising approach for the treatment for type 1 diabetes mellitus. *J Colloid Interface Sci*. (2023) 636:90–102. doi: 10.1016/j.jcis.2022.12.123

162. Hwa AJ, Weir GC. Transplantation of macroencapsulated insulin-producing cells. *Curr Diab Rep*. (2018) 18(8):50. doi: 10.1007/s11892-018-1028-y

163. Brauker JH, Carr-Brendel VE, Martinson LA, Crudele J, Johnston WD, Johnson RC. Neovascularization of synthetic membranes directed by membrane microarchitecture. *J Biomed Mater Res*. (1995) 29(12):1517–24. doi: 10.1002/jbm.820291208

164. Padera RF, Colton CK. Time course of membrane microarchitecture-driven neovascularization. *Biomaterials*. (1996) 17(3):277–84. doi: 10.1016/0142-9612(96)85565-7

165. Geller RL, Loudovaris T, Neuenfeldt S, Johnson RC, Brauker JH. Use of an immunoisolation device for cell transplantation and tumor immunotherapy. *Ann N Y Acad Sci*. (1997) 831:438–51. doi: 10.1111/j.1749-6632.1997.tb52216.x

166. Rafael E, Gazelius B, Wu GS, Tibell A. Longitudinal studies on the microcirculation around the TheraCyte immunoisolation device, using the laser Doppler technique. *Cell Transplant*. (2000) 9(1):107–13. doi: 10.1177/096368970000900113

167. Bowers DT, Song W, Wang LH, Ma M. Engineering the vasculature for islet transplantation. *Acta Biomater*. (2019) 95:131–51. doi: 10.1016/j.actbio.2019.05.051